



β -delayed Fission in r -process Nucleosynthesis

M. R. Mumpower¹, T. Kawano¹, T. M. Sprouse², N. Vassh², E. M. Holmbeck², R. Surman², and P. Möller¹¹Theoretical Division, Los Alamos National Laboratory Los Alamos, NM 87545, USA; mumpower@lanl.gov²Department of Physics, University of Notre Dame Notre Dame, IN 46556, USA

Received 2018 July 24; revised 2018 October 19; accepted 2018 October 21; published 2018 December 6

Abstract

We present β -delayed neutron emission and β -delayed fission (β df) calculations for heavy, neutron-rich nuclei using the coupled Quasi-Particle Random Phase Approximation plus Hauser-Feshbach (QRPA+HF) approach. From the initial population of a compound nucleus after β -decay, we follow the statistical decay, taking into account competition between neutrons, γ -rays, and fission. We find a region of the chart of nuclides where the probability of β df is $\sim 100\%$, which likely prevents the production of superheavy elements in nature. For a subset of nuclei near the neutron dripline, neutron multiplicity and the probability of fission are both large, leading to the intriguing possibility of multi-chance β df, a decay mode for extremely neutron-rich heavy nuclei. In this decay mode, β -decay can be followed by multiple neutron emission, leading to subsequent daughter generations that each have a probability to fission. We explore the impact of β df in rapid neutron-capture process (r -process) nucleosynthesis in the tidal ejecta of a neutron star–neutron star merger and show that it is a key fission channel that shapes the final abundances near the second r -process peak.

Key words: binaries: close – gravitational waves – nuclear reactions, nucleosynthesis, abundances

1. Introduction

One of the greatest challenges in theoretical physics is the determination of the astrophysical location where the heaviest elements on the periodic table are synthesized (Burbidge et al. 1957; Cameron 1957). Solving this problem couples together the quantum theory of nuclei with the description of cataclysmic astrophysical events such as supernovae or merging compact objects (Arnould et al. 2007). Recent gravitational wave and electromagnetic observations suggest that the rapid neutron-capture process (r -process) of nucleosynthesis occurs in the merger of two neutron stars (NSM; Abbott et al. 2017; Cowperthwaite et al. 2017). The r -process in NSMs can create heavy, neutron-rich elements through a series of neutron captures and β -decays among other nuclear reactions (Mumpower et al. 2016b). Many open questions remain regarding the type of conditions that can occur in this environment, but the bulk of the composition of the ejecta is thought to be determined by two primary types of conditions (Kajino & Mathews 2017). The dynamical—or tidally ejected—material flung off at relatively high velocities is expected to be very neutron-rich, capable of producing the actinides that undergo fission (Lattimer & Schramm 1974; Meyer 1989; Freiburghaus et al. 1999). The other type of environment that may be present is a viscous and/or neutrino-driven wind component, which is closer to the center of the merging interface and is believed to have a range of neutron-richness (Surman et al. 2008; Wanajo et al. 2014; Just et al. 2015; Rosswog et al. 2018; Siegel & Metzger 2018). Observations of the GW170817 transient are consistent with the radioactive afterglow of high-opacity, lanthanide-rich material (Tanvir et al. 2017; Kasen et al. 2017). However, it still remains an open question whether actinides were produced. One proposed way to deduce actinide production is to look at the late-time brightness of the kilonova light curve that could be powered by the spontaneous fission of ^{254}Cf (Zhu et al. 2018).

The study of low-electron-fraction ejecta is important, as it opens the possibility to gain insight into unmeasured reactions,

and fission that transmute the heaviest exotic nuclei (Mumpower et al. 2015, 2017). Fission in the r -process is of particular interest; simulations show that an r -process that undergoes multiple fission cycles results in a consistent pattern of abundances between the second and third r -process peaks for a given set of nuclear physics inputs (Beun et al. 2008; Mendoza-Temis et al. 2015). This potentially offers an explanation for the consistent $52 \leq Z \leq 82$ r -process abundance patterns observed in a wide range of stars throughout our galaxy that match the solar r -process pattern (Snedden et al. 2008). The final abundance pattern of a fission recycling r -process is largely shaped by fission properties (Côté et al. 2018): neutron-induced fission rates (Panov & Thielemann 2003; Martínez-Pinedo et al. 2007), spontaneous fission rates (Panov et al. 2013), β -delayed fission probabilities (Thielemann et al. 1983; Ghys et al. 2015), neutrino-induced fission rates (Qian (2002), Kolbe et al. (2004), and fission fragment yields (Goriely et al. 2013; Eichler et al. 2015; Mendoza-Temis et al. 2015; Shibagaki et al. 2016). As noted elsewhere in the literature, fission fragment distributions can have a profound impact on the final abundances of nuclei near the second r -process peak and may also influence the production of rare earth nuclei relative to actinides (Holmbeck et al. 2018). The scission point configuration model of Goriely et al. (2013) exhibits strong multi-peaked yields that are high enough in atomic mass number, A , to appreciably impact the production of lanthanides. The fragment yields of Shibagaki et al. (2016) have one, two, or three component peaks in the mass yield that span a large range ($A \sim 100\text{--}180$), leading to a stark underproduction of the second r -process peak which they hypothesize must be filled in by other contributing nucleosynthetic processes. A smooth trend between symmetric and asymmetric fission yields is given by the two-Gaussian prescription of Kodama & Takahashi (1975) and is used in this paper.

The process of β -delayed fission (β df) is a two-step nuclear decay process that couples β -decay and fission (Andreyev et al. 2013). In β df, a precursor nucleus (Z, A) with Z protons and A nucleons β^\pm -decays into a daughter nucleus ($Z \mp 1, A$) that

has a probability to fission. The study of this low-energy decay mode remains a great challenge experimentally due to the rare branching ratios relative to α -decay (Elseviers et al. 2013; Liberati et al. 2013; Truesdale et al. 2016). For nuclei that may participate in the r -process, β df may be the dominant branching mode due to low fission barriers (Möller et al. 2015). To model the complicated processes after β -decay, we have recently shown that the competition between neutron and γ -ray emission should be included (Mumpower et al. 2016a; Spyrou et al. 2016).

In this paper, we extend our coupled Quasi-Particle Random Phase Approximation and Hauser-Feshbach (QRPA+HF) framework to describe nuclei that may undergo β df. Our treatment leads us to identify a region of the chart of nuclides where the probability of β df is near 100%. This region lies between the neutron dripline and the predicted superheavy island of stability, blocking the decay of r -process species into possibly stable superheavy elements. We discuss a fascinating decay mode for neutron-rich, heavy, r -process nuclei: multi-chance β -delayed fission (mc- β df) in which β -decay may be followed by fission in daughter generations after each stage of neutron emission, similar to multi-chance neutron-induced fission. We show that β df impacts the final abundances of the r -process since it operates on the timescale of β -decay, thus influencing where fission fragments are distributed during the end of fission recycling.

2. Model

The QRPA+HF framework is discussed in Mumpower et al. (2016a) in the context of β -delayed neutron emission. We provide below a brief overview of the model and the necessary enhancement when describing fission. We use this Los Alamos based code, now at version 3.5.0, to follow the statistical de-excitation after β -decay. The code begins with the initial population of a compound nucleus, following Gamow-Teller β -decay treated in the QRPA (Möller et al. 1997) built on top of the 2012 version of the Finite-Range Droplet Model (FRDM2012; Möller et al. 2012, 2016). The subsequent statistical decay of this nucleus is followed, producing output of particle spectra and branching ratios. Standard optical model and γ -strength function choices are used along with a Glibert-Cameron level density with shell corrections included, following the prescription of Ignatyuk (Mumpower et al. 2016a).

When describing nuclei that may fission, an additional transmission coefficient must be calculated. We assume that this transmission coefficient takes the Hill-Wheeler functional form (Hill & Wheeler 1953), representing transmission through a single-hump parabolic barrier dependent on predictions of barrier heights (Möller et al. 2015) with curvature parameter from Thielemann et al. (1983). The level density at the fission saddle point enters into the total fission transmission coefficient in a multiplicative manner, playing a significant role in determining whether or not fission occurs in each daughter generation. The fission level density is larger in deformed configurations than in the ground state due to additional shape degrees of freedom and other collective effects (Bjørnholm 1973; Iljinov et al. 1992).

The statistical de-excitation process is followed in each subsequent daughter generation until all of the initial excitation energy is exhausted. We have found that a good upper bound to the number of daughter generations is 10 neutrons away from

the first daughter nucleus for the most neutron-rich r -process nuclei (Mumpower et al. 2016a). The statistical decay must end in either the population of a daughter generation's ground state or in fission, thus the summation of the probabilities of emitting a neutron or fissioning must be equal to unity:

$$1 = \sum_{j=0}^{10} (P_{jn} + P_{jf}) = P_n + P_f, \quad (1)$$

where P_{jn} is the probability to emit j neutrons, P_{jf} is the probability for the j th compound nucleus to fission, and the cumulative values of these two quantities are denoted P_n and P_f , respectively. Regular β df is defined by $P_{0f} \neq 0$, while mc- β df occurs when $P_{jf} \neq 0$ for $j > 0$, which we describe shortly.

3. Results

We calculate β -delayed neutron emission and fission probabilities using the QRPA+HF framework for all neutron-rich nuclei from stability to extreme neutron excess. The cumulative probability for β df, P_f , is shown in Figure 1 for a subset of these nuclei relevant to the r -process.

There are two key features present in Figure 1 that may have important consequences for r -process nucleosynthesis. The first is the large subset of nuclei beyond the predicted $N = 184$ shell closure in FRDM2012 that have a $P_f = 100\%$, i.e., the β -decay chain always ends in fission rather than the population of the ground state of any β daughter generation, $P_n = 0$. In this region, the nuclear flow of the r -process can no longer increase in proton nuKodama+75mber via β -decay, which can result in termination via β df. This idea was first explored in Thielemann et al. (1983), and we find the β df region in this work extends much further in the NZ -plane and has relatively lower probabilities for nuclei near $(Z, N) \sim (95, 170)$. This extended region of high β df probability may also prevent the production of superheavy elements (near the crossing of the closed shells in Figure 1) in nature, by blocking decay pathways between the r -process path and the island of stability. The thwarting of superheavy element production by regions of high β df probability was also examined in Thielemann et al. (1983); however, only nuclei with proton numbers less than $Z = 100$ (lower than the predicted island of stability) were considered. Older calculations by Meldner (1972), as well as more recent calculations by Petermann et al. (2012), proposed a neutron-rich pathway where nuclei may circumvent fission and subsequently populate superheavy nuclei by chains of β - and α -decays. The extended region of high β df probability in the present work makes this possibility more difficult for the nuclear flow to achieve, a point we return to in the discussion of our nucleosynthesis calculations below.

Very close to the neutron dripline an interesting phenomenon arises. Here, nuclei tend to have very large β -decay Q -values and large neutron multiplicities (on the order of 3–10) in the decay chains toward stability, due to small neutron separation energies (Mumpower et al. 2016a). Since the nuclei along these decay chains have relatively low fission barriers (as predicted with different nuclear potentials (Howard & Möller 1980; Jachimowicz et al. 2017)), it allows the possibility for each of the populated daughter generations to fission after β -decay, $P_{jf} \neq 0$ for some j . We call this phenomenon multi-chance β -delayed fission (mc- β df), analogous to multi-chance neutron-induced fission. This phenomenon can occur in decay chains where neutron multiplicity is greater than zero and there

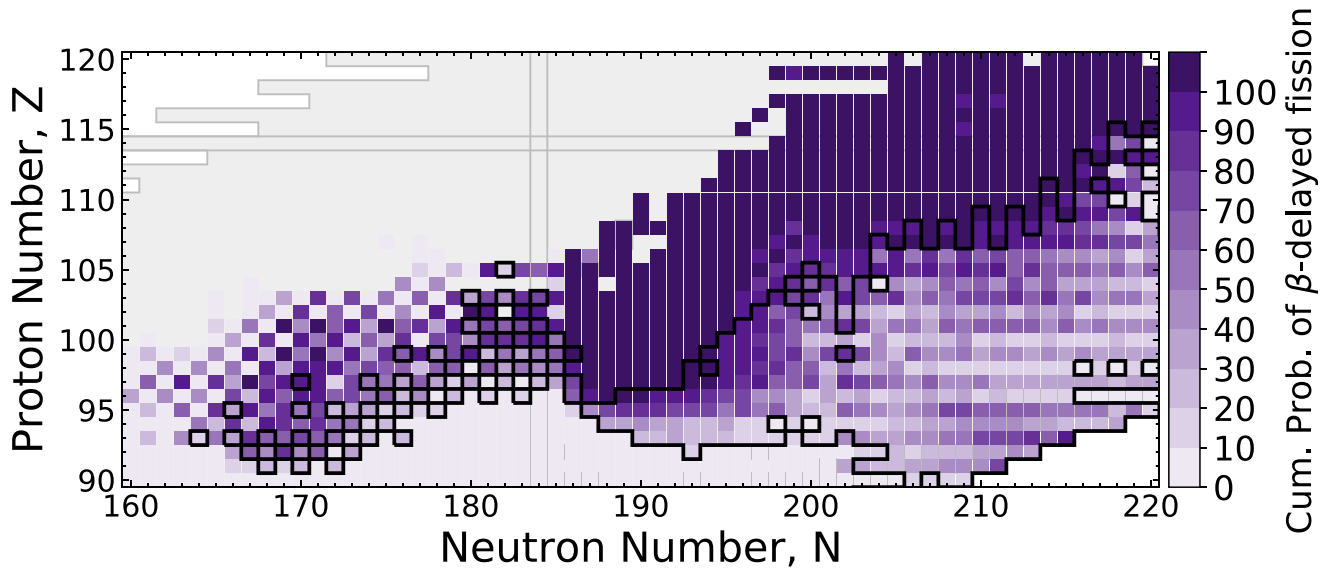


Figure 1. Cumulative probability (P_f) of β df for neutron-rich nuclei using the QRPA+HF framework. The nuclei that exhibit mc- β df are outlined in a black bounding box. Gray shading denotes nuclei that are bound by proton or neutron emission in FRDM2012 and have $P_f = 0$.

is sufficient cumulative probability to fission. We define this constraint to be $\sum_{j=1}^{10} P_{jf} \geq 10\%$, with the $j = 0$ component or regular β df left out of the summation. The nuclei that exhibit mc- β df are a subset of the most neutron-rich nuclei that are predicted to undergo β df, occupying roughly half of the β df “real estate” toward the uncertain location of the neutron dripline (Erler et al. 2012). The existence of mc- β df is the second key feature of Figure 1 that can impact the r -process. Rather than only considering the daughter ($j = 0$) that fissions, as in β df, each possible daughter generation ($j > 0$) may fission. Thus, the population of light nuclei during the r -process from this fission channel is actually a superposition of fission fragment yields of a chain of all the daughter nuclei.

To gauge the impact of the β df properties, we perform r -process nuclear network calculations using version 2.0 of PRISM (Portable Routines for Integrated nucleoSynthesis Modeling; Mumpower et al. 2017; Côté et al. 2018; T. Sprouse & M. R. Mumpower 2018, in preparation) based off FRDM2012 nuclear properties. Standard r -process reaction channels are included along with the β df rates and branching ratios from this work. The reaction rates of r -process nuclei are calculated using the LANL statistical Hauser-Feshbach code of Kawano et al. (2016). Fission fragment distributions of Kodama & Takahashi (1975; K&T) are used for neutron-induced, beta-delayed, and spontaneous fission (spf) yields unless stated otherwise. Evaluated data from NUBASE2016 (Audi et al. 2017), including measured spf rates, and measured masses from the AME2012 (Audi et al. 2012), are used when available. For astrophysical conditions, we choose neutron star merger trajectories corresponding to the “slow” neutron-rich dynamical ejecta of Mendoza-Temis et al. (2015), as well as the low entropy ($s \sim 10$) with very low initial electron fraction ($Y_e \sim 0.01$) dynamical ejecta from Goriely et al. (2011).

In order to address the effects of heating from fission, as well as nuclear reactions and decays, PRISM implements an equation of state based on the Helmholtz equation of state (Timmes & Arnett 1999; Timmes & Swesty 2000), treating electrons and positrons as arbitrarily relativistic and degenerate non-interacting Fermi gases and photons as blackbody

radiation. PRISM additionally treats the population of each nuclear species as a Maxwell–Boltzmann gas, with all thermodynamic quantities calculated using the same nuclear data as was used to calculate nuclear reaction and decay properties as described above. The amount of heat introduced over each time step is assumed to be a 10% fraction of all nuclear energy released over the same time step, and the consequent changes in both entropy and temperature are updated for the following time step using this equation of state. The evolution of density is taken at all time steps to be the same as in the original trajectories.

In the initially low entropy conditions studied here, fission processes can contribute significantly to the heating of the ejecta primarily from the large Q -values (~ 200 MeV) and substantial flow through the participating nuclei. Additional prompt particle or gamma-ray emission would reduce the fission Q -values, but this is in general only on the order of 10%. In response to the energy release, the entropy of the material will increase rapidly during this period of time, with corresponding effects on the temperature. PRISM employs a hybrid implicit-explicit method to consistently update the entropy and temperature throughout the calculation, similar to that of Lippuner & Roberts (2017).

First, we consider the possible production of superheavy elements in our r -process calculations. For all example calculations considered we find that neutron-induced fission rates calculated with FRDM2012 masses and barrier heights can alone prevent the formation of superheavy elements, in agreement with Boleu et al. (1972), Howard & Nix (1974), and Petermann et al. (2012). In such calculations, neutron-induced fission terminates the r -process around $A \approx 290$, lower than the crossing of the shell closures in Figure 1. However, astrophysical capture rates can vary by several orders of magnitude, so it is important to consider the effect of β df alone (e.g., in the absence of neutron-induced fission). We repeat our network calculations with only the β df and experimental spf (Audi et al. 2017) channels included and show the evolution of r -process abundances in Figure 2. Figure 2 demonstrates that $A \gtrsim 290$ nuclei are (a) populated at a time before the nuclear flow encounters the region from Figure 1 with a β df probability

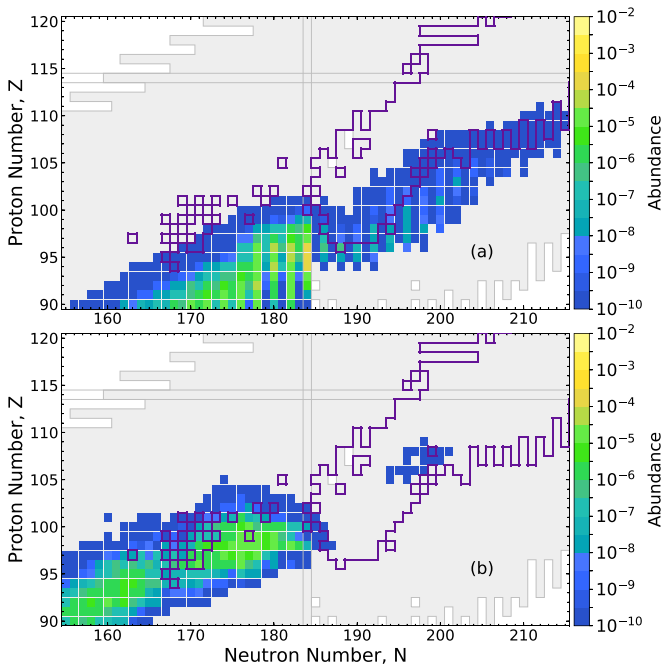


Figure 2. r -process abundances at a time (a) just before the nuclear flow encounters the $P_f \geq 90\%$ region from Figure 1 (outlined in purple) and (b) after encountering this high-probability β df region. The network calculations shown here include only β df and experimental sp f channels and are for astrophysical conditions from Mendoza-Temis et al. (2015).

$\geq 90\%$ and (b) not populated after moving through this high-probability β df region. Therefore, even in the absence of neutron-induced fission, β df is itself sufficient to prevent the production of superheavy nuclei by blocking decay pathways to stability.

As indicated above, our calculations show that when all fission channels are included, the r -process terminates via neutron-induced fission. It might be expected, then, that neutron-induced fission is largely responsible for shaping the final r -process abundance pattern. To show an example of how β df can influence the r -process pattern, we apply two different fission fragment distribution schemes. In the first, we replace the K&T fission fragment distribution of the neutron-induced fission yields with a simple, symmetric split that assigns an atomic mass number half that of the fissioning system to each of the fragments (and no neutrons are emitted). The β df fragments retain the K&T yields (β df K&T). For the second fission scheme, we use simple symmetric splits for both neutron-induced fission and β df channels (β df Ss.). When applied to all fissioning nuclei, a simple symmetric split produces an abundance pattern in which the fission products are deposited directly in the $A \sim 130$ region, leading to a sharp, well-defined second r -process peak as shown by the solid line in Figure 3. The K&T yields, on the other hand, use a double Gaussian distribution, placing fission products in a wide range of nuclei resulting in a broader second peak that extends over a range of atomic mass number. If neutron-induced fission dominated at all times, the effect of changing the β df fragment distribution would be small and the abundance patterns with the two fission schemes would be similar. The clear signature of the K&T yields appears with the β df K&T scheme, indicating the β df channel plays a key role in shaping the $A \sim 130$ peak. To make this comparison more precise, we compute a quantitative metric for the difference between these

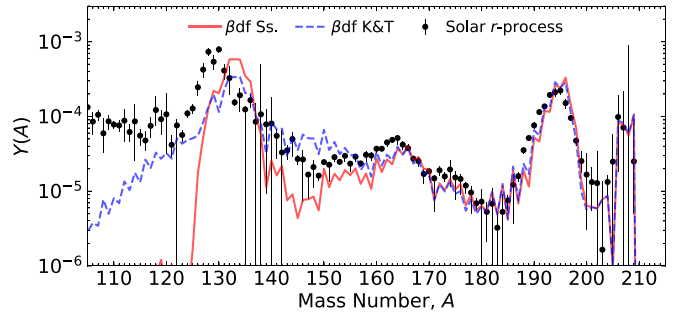


Figure 3. Final abundances of a neutron-star merger trajectory (Goriely et al. 2011) at 1 Gyr using 50/50 symmetric fission yields (solid), as compared to the yield distribution of K&T (dashed) for the β df channel. Solar data from Sneden et al. (2008) are shown in black dots.

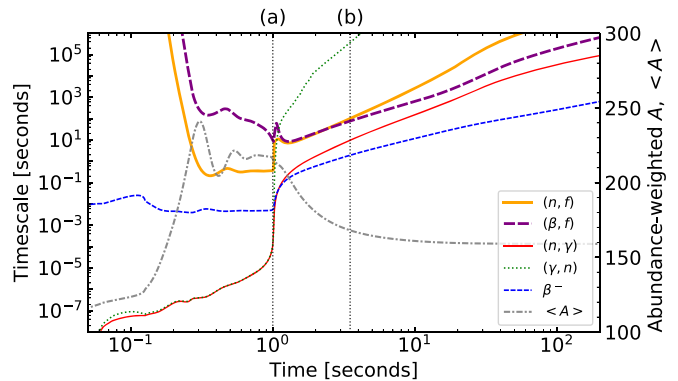


Figure 4. Selection of abundance-weighted timescales vs. time for the r -process phase of a neutron-star merger event (Goriely et al. 2011). The vertical line (a) indicates the time at which neutron-capture falls out of equilibrium, while the vertical line (b) demarks the point when the β df timescale is faster than the timescale for neutron-induced fission.

two patterns, with our choice of metric being the commonly used F from sensitivity studies (Mumpower et al. 2016b). The F -value for these two calculations is 36.27, which represents a large global change between the final abundance patterns.

The precise mechanism of this influence can be understood from an investigation of the r -process dynamics (Mumpower et al. 2012). Figure 4 shows the relative importance of select nuclear reaction channels as the r -process proceeds in neutron-rich conditions. The early r -process is characterized by (n, γ) – (γ, n) equilibrium. The onset of fission recycling is indicated by the peak in the abundance-weighted average A , shown by the dotted-dashed line in Figure 4. During these early times, neutron-induced fission dominates fission recycling, and it continues to be the primary fission channel throughout most of the fission recycling phase for these astrophysical conditions. As (n, γ) – (γ, n) fails, indicated in Figure 4 by the left vertical dashed line (a) at $t \sim 1$ s, a competition between neutron-capture and β -decay arises. At this stage, the neutron abundance drops rapidly and thus fission fragments cannot change significantly in A via neutron captures as they decay back to stability. At about $t \sim 2.3$ s, the right vertical dashed line labeled (b) in Figure 4 β df becomes the primary fission channel while nuclei are decaying. Thus, the late stage or final fission cycle, which is increasingly dominated by β df, will dictate the final form of the abundances of lighter-mass nuclei near the $A = 130$ peak, as supported by Figure 3.

We now show that mc- β df is an integral part of the β df channel by looking at the relative fission flows. Reaction flows,

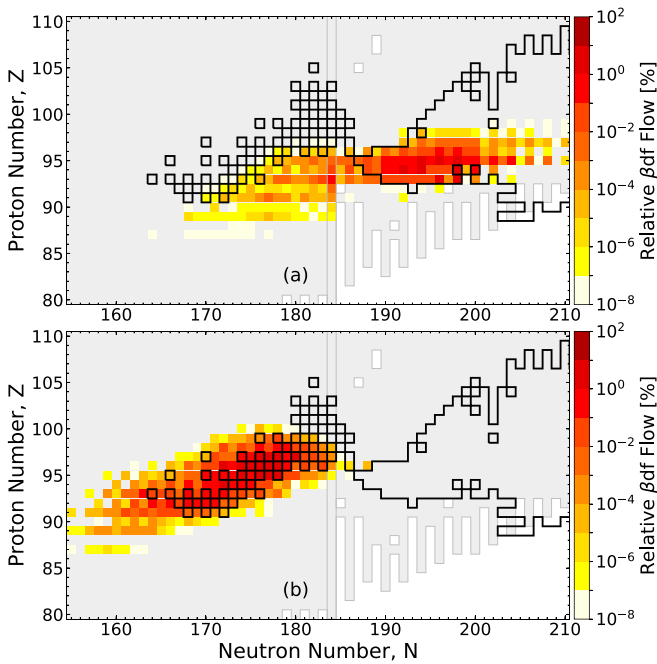


Figure 5. Relative β df flow compared to the total fission flow at an early time (a) when neutron-induced fission dominates and at a later time (b) when β df becomes dominant. Selected times correspond to the dotted vertical lines in Figure 4. At both times, mc- β df exhibits large flow, which is indicated by the black region (similar to Figure 1).

$\mathcal{F} = Y(Z, N) \times \lambda$, where $Y(Z, N)$ is the abundance and λ is the rate in s^{-1} , permit an observation of the hotspots for particular reaction channels in the NZ -plane. In Figure 5 we examine the β df flows, denoted $\mathcal{F}(Z, N)_{\beta, f}$, at an early and late time in the r -process evolution. The colors indicate the relative β df flow, $\mathcal{F}(Z, N)_{\beta, f} / \dot{Y}_f$, where $\dot{Y}_f = \sum_{Z, N} [\mathcal{F}(Z, N)_{\beta, f} + \mathcal{F}(Z, N)_{n, f}]$ is the total fission flow of all nuclei in the network at a given time, with $\mathcal{F}(Z, N)_{n, f}$ representing the neutron-induced fission flow. We neglect spontaneous fission in this sum since it is not expected to substantially contribute far from stability using parameterized models, e.g., from Zagrebaev & Greiner (2011), and Petermann et al. (2012), on the timescale of interest for neutron-induced or β df. The region where the cumulative mc- β df probability exceeds 10% (as described in Figure 1) is outlined in Figure 5 in black. Nuclei exhibiting mc- β df are active both at early times when neutron-induced fission contributes significantly (a), and at later times, when the neutron flux has been exhausted and the β df channel begins to dominate (b). Since the bulk of the high-mass flow goes through the mc- β df region, mc- β df contributes significantly to the β df flow until very late times in the simulation. It is only once the r -process path has drawn closer to stability that first-chance β df takes over.

A substantial amount of energy is released from the radioactive decay of r -process nuclei. The fraction of this energy released that thermalizes with the ejected material can be re-radiated as thermal emission, powering a light curve; see, e.g., (Barnes et al. 2016; Kasen et al. 2017; Tanvir et al. 2017) and references therein. While the calculation of an associated light curve with our nucleosynthesis model is beyond the scope of this work, we point out that the β df channel can contribute to the fraction of heating that occurs on the timescale of a day, as shown in Figure 6. The impact of first-chance β df stems from both the long timescale over which the channel may operate

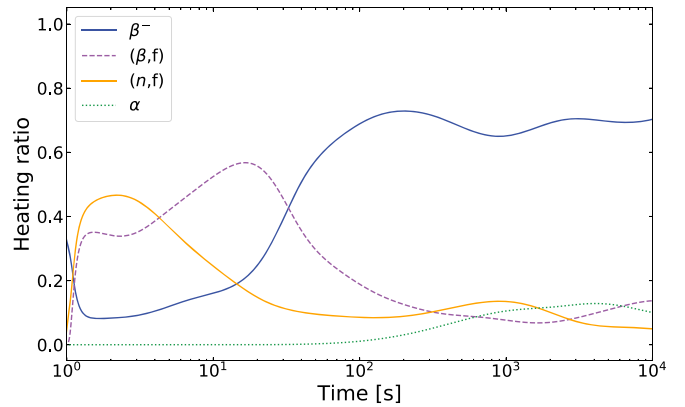


Figure 6. Ratio of late-time heating channels relevant for a kilonova light curve for the trajectory of Goriely et al. (2011). The β df channel can contribute a notable fraction of the total heating curve.

(recall Figure 4), as well as the large Q -value (~ 200 MeV) corresponding with the fission process. From previous discussions it is clear that mc- β df will play less of a role in heating, since these nuclei exhibit relatively short half-lives. The efficiency with which fission products thermalize is high, even on the order of days. Thus, if the region of β df is reached in an r -process trajectory, it is reasonable to expect that this channel will contribute to the radioactive glow known as a kilonova (Metzger et al. 2010).

4. Conclusions

In summary, we have extended the QRPA+HF framework to describe β -delayed fission (β df) for nuclei that may participate in neutron-rich heavy element nucleosynthesis. We isolated a region of nuclear chart with β df probability near 100% that has an extended range in proton number and demonstrated that this region can prevent the formation of the superheavy elements in nature by the r -process. We have identified an important decay mode, multi-chance β -delayed fission (mc- β df), that can contribute to the β df flow in the dynamical ejecta of a neutron star merger r -process and therefore impact the final abundances near the second r -process peak. Current calculations of fission rates and yields, including this work, assume independence between these quantities, representing a clear barrier to progress in understanding light element abundances that may be influenced by fission products. We plan to address this issue in an upcoming publication where all fission properties will stem from the Finite-Range Liquid-Drop Model.

The authors thank Oleg Korobkin, Chris Fryer, and Kohji Takahashi for useful discussions. This work was supported in part by the FIRE (Fission In R -process Elements) collaboration (M.M., T.K., N.V., and R.S.). M.M., T.K., and P.M. were supported by the National Nuclear Security Administration of the U.S. Department of Energy at Los Alamos National Laboratory under contract No. DE-AC52-06NA25396. T.M.S., E.M.H., and R.S. were supported by U.S. Department of Energy contract No. DE-SC0013039. T.M.S. was additionally supported by U.S. Department of Energy SciDAC grant DE-SC0018232.

ORCID iDs

M. R. Mumpower  <https://orcid.org/0000-0002-9950-9688>
 T. Kawano  <https://orcid.org/0000-0001-7463-4899>
 T. M. Sprouse  <https://orcid.org/00000-0002-4375-4369>
 N. Vassh  <https://orcid.org/0000-0002-3305-4326>
 E. M. Holmbeck  <https://orcid.org/0000-0002-5463-6800>
 R. Surman  <https://orcid.org/0000-0002-4729-8823>
 P. Möller  <https://orcid.org/0000-0002-5848-3565>

References

- Abbott, B. P., Abbott, R., Abbott, T. D., et al. 2017, *PhRvL*, **119**, 161101
 Andreyev, A. N., Huyse, M., & Van Duppen, P. 2013, *RvMP*, **85**, 1541
 Arnould, M., Goriely, S., & Takahashi, K. 2007, *PhR*, **450**, 97
 Audi, G., Kondev, F., Wang, M., Huang, W., & Naimi, S. 2017, *ChPhC*, **41**, 030001
 Audi, G., Wang, M., Wapstra, A. H., et al. 2012, *ChPhC*, **36**, 2
 Barnes, J., Kasen, D., Wu, M.-R., & Martínez-Pinedo, G. 2016, *ApJ*, **829**, 110
 Beun, J., McLaughlin, G. C., Surman, R., & Hix, W. R. 2008, *PhRvC*, **77**, 035804
 Bjørnholm 1973, in Proc. 3rd Symp., Physics and Chemistry of Fission (Vienna: IAEA)
 Boleu, R., Nilsson, S. G., Sheline, R. K., & Takahashi, K. 1972, *PhLB*, **40**, 517
 Burbidge, E. M., Burbidge, G. R., Fowler, W. A., & Hoyle, F. 1957, *RvMP*, **29**, 547
 Cameron, A. G. W. 1957, Chalk River Reports, Nuclear Reactions in Stars and Nucleogenesis, CRL-41
 Côté, B., Fryer, C. L., Belczynski, K., et al. 2018, *ApJ*, **855**, 99
 Cowperthwaite, P. S., Berger, E., Villar, V. A., et al. 2017, *ApJL*, **848**, L17
 Eichler, M., Arcones, A., Kelic, A., et al. 2015, *ApJ*, **808**, 30
 Elseviers, J., Andreyev, A. N., Huyse, M., et al. 2013, *PhRvC*, **88**, 044321
 Erler, J., Birge, N., Kortelainen, M., et al. 2012, *Natur*, **486**, 509
 Freiburghaus, C., Rosswog, S., & Thielemann, F.-K. 1999, *ApJL*, **525**, L121
 Ghys, L., Andreyev, A. N., Antalic, S., Huyse, M., & Van Duppen, P. 2015, *PhRvC*, **91**, 044314
 Goriely, S., Bauswein, A., & Janka, H.-T. 2011, *ApJL*, **738**, L32
 Goriely, S., Sida, J.-L., Lemaître, J.-F., et al. 2013, *PhRvL*, **111**, 242502
 Hill, D. L., & Wheeler, J. A. 1953, *PhRv*, **89**, 1102
 Holmbeck, E. M., Surman, R., Sprouse, T. M., et al. 2018, arXiv:1807.06662
 Howard, W. M., & Möller, P. 1980, *ADNDT*, **25**, 219
 Howard, W. M., & Nix, J. R. 1974, *Natur*, **247**, 17
 Ijtinov, A. S., Mebel, M. V., Bianchi, N., et al. 1992, *NuPhA*, **543**, 517
 Jachimowicz, P., Kowal, M., & Skalski, J. 2017, *PhRvC*, **95**, 014303
 Just, O., Bauswein, A., Pulpillo, R. A., Goriely, S., & Janka, H.-T. 2015, *MNRAS*, **448**, 541
 Kajino, T., & Mathews, G. J. 2017, *RPPH*, **80**, 084901
 Kasen, D., Metzger, B., Barnes, J., Quataert, E., & Ramirez-Ruiz, E. 2017, *Natur*, **551**, 80
 Kawano, T., Capote, R., Hilaire, S., & Chau Huu-Tai, P. 2016, *PhRvC*, **94**, 014612
 Kodama, T., & Takahashi, K. 1975, *NuPhA*, **239**, 489
 Kolbe, E., Langanke, K., & Fuller, G. M. 2004, *PhRvL*, **92**, 111101
 Lattimer, J. M., & Schramm, D. N. 1974, *ApJL*, **192**, L145
 Liberati, V., Andreyev, A. N., Antalic, S., et al. 2013, *PhRvC*, **88**, 044322
 Lippuner, J., & Roberts, L. F. 2017, *ApJS*, **233**, 18
 Martínez-Pinedo, G., Mochel, D., Zinner, N., et al. 2007, *PrPNP*, **59**, 199
 Meldner, H. W. 1972, *PhRvL*, **28**, 975
 Mendoza-Temis, J. D. J., Wu, M.-R., Langanke, K., et al. 2015, *PhRvC*, **92**, 055805
 Metzger, B. D., Martínez-Pinedo, G., Darbha, S., et al. 2010, *MNRAS*, **406**, 2650
 Meyer, B. S. 1989, *ApJ*, **343**, 254
 Möller, P., Myers, W. D., Sagawa, H., & Yoshida, S. 2012, *PhRvL*, **108**, 052501
 Möller, P., Nix, J. R., & Kratz, K.-L. 1997, *ADNDT*, **66**, 131
 Möller, P., Sierk, A. J., Ichikawa, T., Iwamoto, A., & Mumpower, M. 2015, *PhRvC*, **91**, 024310
 Möller, P., Sierk, A. J., Ichikawa, T., & Sagawa, H. 2016, *ADNDT*, **109**, 1
 Mumpower, M. R., Kawano, T., & Möller, P. 2016a, *PhRvC*, **94**, 064317
 Mumpower, M. R., McLaughlin, G. C., & Surman, R. 2012, *PhRvC*, **85**, 045801
 Mumpower, M. R., McLaughlin, G. C., Surman, R., & Steiner, A. W. 2017, *JPhG*, **44**, 034003
 Mumpower, M. R., Surman, R., Fang, D.-L., et al. 2015, *PhRvC*, **92**, 035807
 Mumpower, M. R., Surman, R., McLaughlin, G. C., & Aprahamian, A. 2016b, *PrPNP*, **86**, 86
 Panov, I., & Thielemann, F.-K. 2003, *NuPhA*, **718**, 647
 Panov, I. V., Korneev, I. Y., Martínez-Pinedo, G., & Thielemann, F.-K. 2013, *AstL*, **39**, 150
 Petermann, I., Langanke, K., Martínez-Pinedo, G., et al. 2012, *EPJA*, **48**, 122
 Qian, Y.-Z. 2002, *ApJL*, **569**, L103
 Rosswog, S., Sollerman, J., Feindt, U., et al. 2018, *A&A*, **615**, A132
 Shibagaki, S., Kajino, T., Mathews, G. J., et al. 2016, *ApJ*, **816**, 79
 Siegel, D. M., & Metzger, B. D. 2018, *ApJ*, **858**, 52
 Sneden, C., Cowan, J. J., & Gallino, R. 2008, *ARA&A*, **46**, 241
 Spyrou, A., Liddick, S. N., Naqvi, F., et al. 2016, *PhRvL*, **117**, 142701
 Surman, R., McLaughlin, G. C., Ruffert, M., Janka, H.-T., & Hix, W. R. 2008, *ApJL*, **679**, L117
 Tanvir, N. R., Levan, A. J., González-Fernández, C., et al. 2017, *ApJL*, **848**, L27
 Thielemann, F.-K., Metzinger, J., & Klapdor, H. V. 1983, *ZPhyA*, **309**, 301
 Timmes, F. X., & Arnett, D. 1999, *ApJS*, **125**, 277
 Timmes, F. X., & Swesty, F. D. 2000, *ApJS*, **126**, 501
 Triesdale, V. L., Andreyev, A. N., Ghys, L., et al. 2016, *PhRvC*, **94**, 034308
 Wanajo, S., Sekiguchi, Y., Nishimura, N., et al. 2014, *ApJL*, **789**, L39
 Zagrebaev, V. I., & Greiner, W. 2011, *PhRvC*, **83**, 044618
 Zhu, Y., Wollaeger, R. T., Vassh, N., et al. 2018, *ApJL*, **863**, L23